Log Number: 560

STUDY OF SUPERCRITICAL CARBON DIOXIDE NATURAL CIRCULATION BY THE USE OF CFD CODES

E. Molfese¹, W. Ambrosini¹, N. Forgione¹, P.K. Vijayan² and M. Sharma²

¹ University of Pisa, Dipartimento di Ingegneria Meccanica Nucleare e della Produzione, Italy

² Reactor Engineering Division, Bhabha Atomic Research Centre, Mumbai, India

w.ambrosini@ing.unipi.it, n.forgione@ing.unipi.it, vijayanp@barc.gov.in, manishs@barc.gov.in

Abstract

In this paper, experiments on natural circulation of CO₂, previously performed at the Bhabha Atomic Research Centre (BARC), are addressed by the use of the FLUENT and the STAR-CCM+ CFD codes. The experiments were carried out in an experimental facility installed at the Reactor Engineering Division of BARC in Mumbai, consisting in a uniform diameter (13.88 mm ID & 21.34 mm OD) rectangular loop (SCNCL) with different orientations of heater and cooler, which can operate with either supercritical water and supercritical carbon dioxide. The tests with carbon dioxide were performed at different power levels, at the supercritical pressures of 8.6 and 9.1 MPa. The steady-state characteristics of the loop were obtained for the horizontal heater and the horizontal cooler configuration (HHHC) and for the horizontal heater and vertical cooler one (HHVC). Unstable behaviour was observed only for the HHHC configuration. The FLUENT and the STAR-CCM+ codes were adopted for reproducing the observed behaviour of the experimental loop in the HHHC configuration. Steady-state as well as transient analyses were performed to be compared with the observed behaviour of the loop.

1. Introduction

The SCWR concept envisages that the cooling and moderation of the core (for the thermal neutron spectrum option) is accomplished by light water at pressures higher than the critical one (hence the adjective "supercritical") [1-3]. The use of light water at supercritical pressures (e.g., at 25 MPa) avoids boiling (no phase change between liquid and gas) and therefore the outlet core temperature can be raised considerably (up to 550 °C) as there is no risk of a thermal crisis, in favour of higher conversion efficiencies, evaluated to be up to 45%.

Though it is basically a single-phase fluid, the large enthalpy change possible in supercritical water reduces the coolant flow rate as well as the pumping power, while the adoption of a direct cycle simplifies the nuclear system, eliminating the need of recirculation lines, pressurizer, heat exchanger, steam separators and dryers. In summary, the SCWR design takes advantage of the very desirable feature of the Boiling Water Reactors (BWRs) with respect to the Pressurized Water Reactors (PWRs), being the direct cycle, without the associated disadvantage of dealing with a two-phase flow system in normal operation, with all the associated complications.

Nevertheless, though there are large benefits from the employment of SCWRs, the design difficulties and technological challenges, mainly in terms of material resistance, together with the need to get reliable models for the physical phenomena occurring with supercritical fluids, require a significant effort in terms of research and development. Indeed, in supercritical water reactor operating conditions, the thermodynamic and transport properties of water change remarkably as the temperature approaches the "pseudocritical point", corresponding to a sharp maximum observed in specific heat at each working pressure.

As an example, the large changes in density, similar in magnitude to those encountered during boiling, make the SCWR core susceptible to flow instabilities similar to those observed in BWRs (such as density-wave instabilities and coupled neutronic thermo-hydraulic instabilities). Since the operation with unstable flow is highly undesirable, as it can lead to power oscillations, causing mechanical vibration of components and challenging the control system, the deployment of SCWRs is conditioned to the design of stable systems. In this aim, it is necessary to clearly understand and predict the instability phenomena occurring with supercritical fluids and to identify the variables which affect these phenomena.

Natural circulation is known to be a relevant phenomenon for nuclear reactors since it involves several regimes of reactor operation. Though the natural circulation phenomena at subcritical pressure, both in single and two-phase flows, have been thoroughly studied, the same cannot be said for natural circulation with supercritical fluids. Indeed, very few experimental studies on natural circulation with supercritical fluids are reported in previous literature (see e.g., [4]).

The University of Pisa, Italy, and the Bhabha Atomic Energy Centre (BARC) of Mumbai, India, are both involved in the Coordinated Research Project (CRP) of the International Atomic Energy Agency (IAEA) on "Heat Transfer Behaviour and Thermo-hydraulics Codes Testing for SCWRs". This IAEA CRP promotes international collaboration among IAEA Member States (Usa, Russia, China, UK, Canada, India, Italy and other Countries) with the aim to collect accurate data on heat transfer, pressure drops, natural convection and stability regarding fluids at supercritical pressure, as well as to develop reliable thermal-hydraulic codes for SCWRs.

In the framework of this co-operation, the experimental data obtained at the BARC, related to natural circulation with CO_2 at supercritical pressures, were used in this work to test the predictions of two different CFD codes: Fluent [5] and STAR-CCM+ [6].

The study addressed most of the experimental information made available in the experimental research, involving steady-state as well as transient analyses for supercritical CO₂ [7]; the actual operating conditions of the experiments, as well as various others like "open loop" and "closed loop" configurations with imposed cooling flux, were considered in order to provide an overview of the capabilities of available computational tools in predicting natural circulation phenomena. However, only the operating conditions directly related to performed experiments will be discussed herein.

2. The Experimental Facility

In Figure 1, the schematic of the SPNCL experimental loop installed at BARC is reported [7]. It is a uniform diameter rectangular loop made of 13.88 mm inside diameter stainless steel (SS-347) pipe, with an outside diameter of 21.34 mm. The loop has two heated sections and two cooler sections, so that it can be operated in any one of the four orientations such as Horizontal Heater Horizontal Cooler (HHHC), Horizontal Heater Vertical Cooler (HHVC), Vertical Heater Horizontal Cooler (VHHC) and Vertical Heater Vertical Cooler (VHVC).

The heater was made by uniformly winding nichrome wire over a layer of fiber glass insulation. The cooler was of the tube-in-tube type with chilled water as the secondary coolant flowing in the annulus. The outer tube forming the annulus had a 77.9 mm inside diameter and 88.9 mm outside diameter. The loop had a pressurizer connected to the bottom horizontal pipe which allows for thermal expansion, besides accommodating the cover gas helium above the carbon dioxide. The safety devices of the loop (i.e. rupture discs RD-1 & RD-2) were installed on top of the pressurizer which also had provision for CO_2 and He filling. The entire loop was insulated with three inches of ceramic mat (k=0.06 W/(mK)).

The loop was instrumented with 44 calibrated K-type mineral insulated thermocouples (1 mm diameter) to measure the primary fluid, secondary fluid and heater outside wall temperatures. Primary fluid temperatures at each location were measured as the average value indicated by two thermocouples inserted diametrically opposite at a distance of r/2 from the inside wall. On the other hand, secondary fluid temperatures were measured by a single thermocouple located at the tube centre. This was adequate to obtain the average temperature as the temperature increase in the secondary fluid was small (< 4 °C). The thermocouples used to measure the heater outside wall temperature were installed flush with the outside surface for a total of 12 thermocouples placed at six axial distances at diametrically opposite locations.

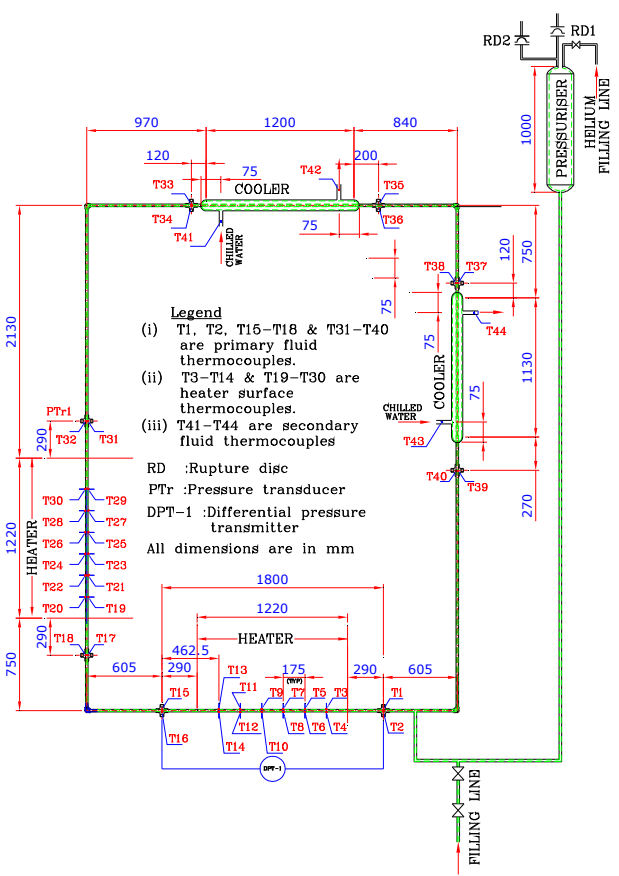


Figure 1. Schematic of the supercritical pressure natural circulation loop (SPNCL) of the BARC

Tests were performed to quantify the heat losses and the pressure drops along the loop. The pressure drop characterization tests were carried out under forced flow conditions with the help of a pump in a separate facility using the same bottom horizontal pipe and one of the elbows installed horizontally. From the measured pressure drop across the bottom horizontal pipe and the flow rate, the friction factor for the pipe was estimated. Figure 2 reports the obtained data together with the correlation fitted to them; from the measured pressure drop across the elbow and the flow rate, the loss coefficient was also estimated, as reported in the same figure.

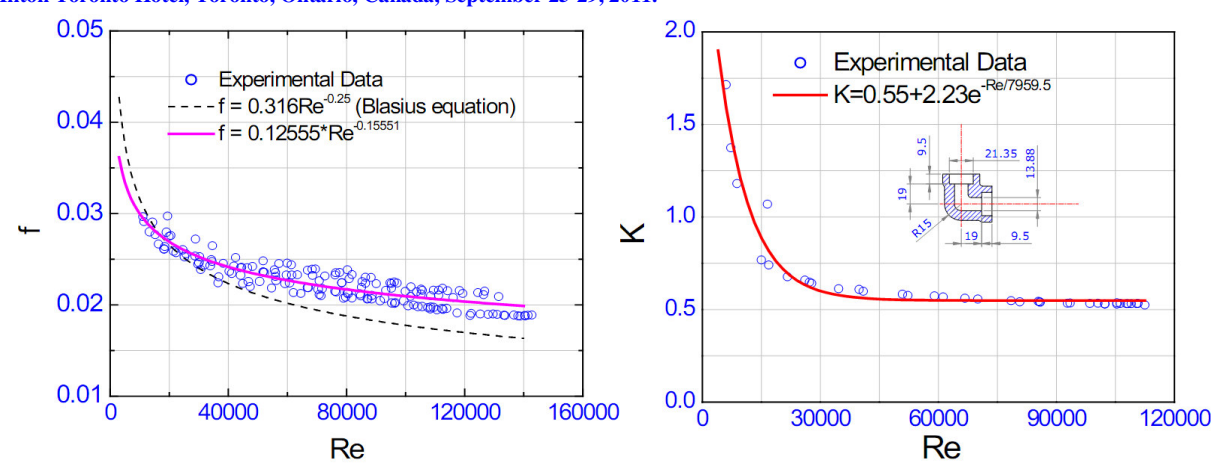


Figure 2. Experimental values of friction factor and elbow K coefficient

To estimate the heat losses, natural circulation experiments were carried out at various powers with water at subcritical conditions. These experiments were performed at a system pressure of 30 bar for all the four orientations of the heater and cooler. Since the ambient temperature was significantly high (30 ± 2 °C) compared to the chilled water coolant temperature (9.8 ± 1.6 °C), in certain low power cases heat was gained rather than lost. Figure 3 reports the data obtained in the different configurations.

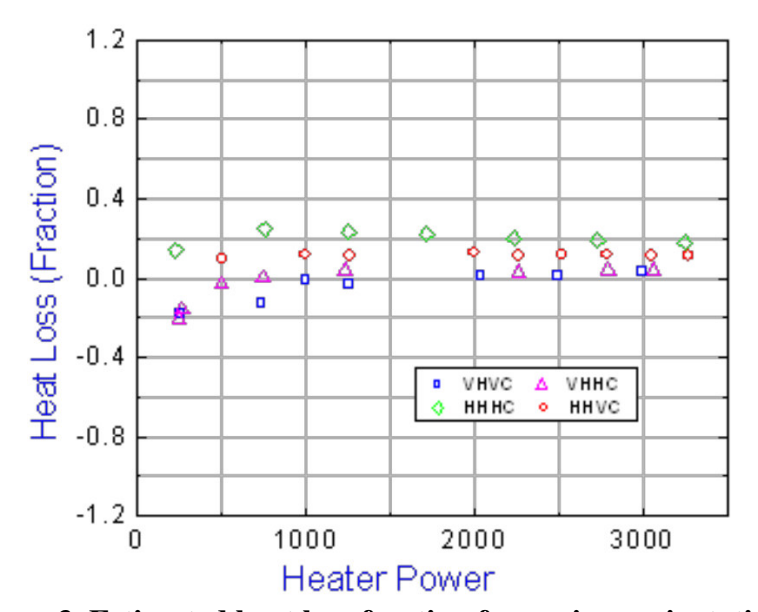


Figure 3. Estimated heat loss fraction for various orientations during NC experiments with subcritical water

Log Number: 560

3. Addressed Experimental tests

Before operation with supercritical CO₂, the loop was flushed repeatedly with CO₂ at low pressure including all impulse, drain and vent lines. Subsequently the loop was filled with CO₂ up to 50 bar in pressure and the chilled water coolant was valved in. This caused condensation of CO₂ and hence a decrease in loop pressure. The pressure decrease was compensated by admitting additional CO₂ from the cylinder and again allowing sufficient time for condensation. The process of filling and condensation was continued till there was no decrease in pressure.

At this point the loop pressure was increased to the required value with the help of a helium gas cylinder. Once the required supercritical pressure was achieved, the helium cylinder was isolated. Sufficient time was allowed to reach a steady state. It was found difficult to attain completely stagnant conditions with uniform temperature throughout the loop as the higher ambient temperature allowed a small amount of heat absorption through the insulation into the loop which was rejected at the cooler causing a small circulation rate.

Once a steady state was achieved, the heater power was switched on and adjusted at the required value. Sufficient time was allowed to achieve the steady state. Once the steady state was achieved, power was increased and again sufficient time was provided to achieve the steady state. In case the system pressure increased beyond the set value by 1 bar, a little helium was vented out to bring back the pressure to the original value. Similarly during power decrease if the pressure decreases below the set point by one bar, then the loop was pressurized by admitting additional helium into the pressurizer.

The experiments were repeated for different pressures and different chilled water flow rates. Subsequently the experiments were performed for different orientations of the heater and the cooler.

Steady-state data on natural circulation flow rate and heat transfer were generated with supercritical CO_2 for various orientations of the source and sink. The range of parameters of all the steady state data is the following:

- Orientations studied: HHHC, HHVC, VHHC and VHVC;
- Pressure: 8 9.2 MPa;
- Power: 0.1 2.4 kW;
- Cold leg temperature: 17.5 57.7 °C;
- Hot leg temperature: 19.3 95.9 °C;
- Coolant flow rate: 29.6 56 lpm (liters per minute);
- Coolant inlet temperature: 8.2 11.4 °C;
- Coolant outlet temperature: 9.0 12.5 °C.

The steady state mass flow rate was estimated using the measured heater power and the enthalpy rise across the heater, estimating the enthalpies at the heater inlet and outlet using the corresponding measured temperatures and the system pressure. The flow rate data across the pseudocritical region are to be considered less reliable than those outside, because in the pseudocritical region a greater error can be obtained in estimating the fluid enthalpy due to the sharp change of specific heat (see Figure 4). The flow rates so estimated were compared with the predictions of the in-house developed computer code NOLSTA [8] and the results are presented in Figure 5.

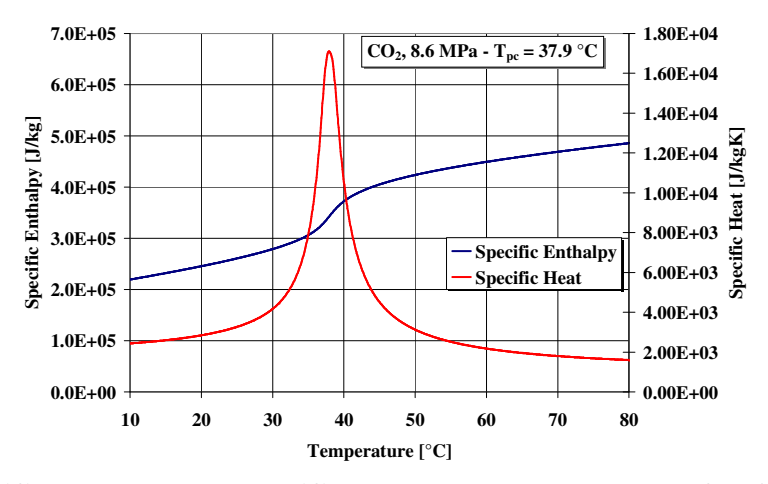


Figure 4. Specific enthalpy and specific heat at constant pressure for CO₂ at 8.6 MPa

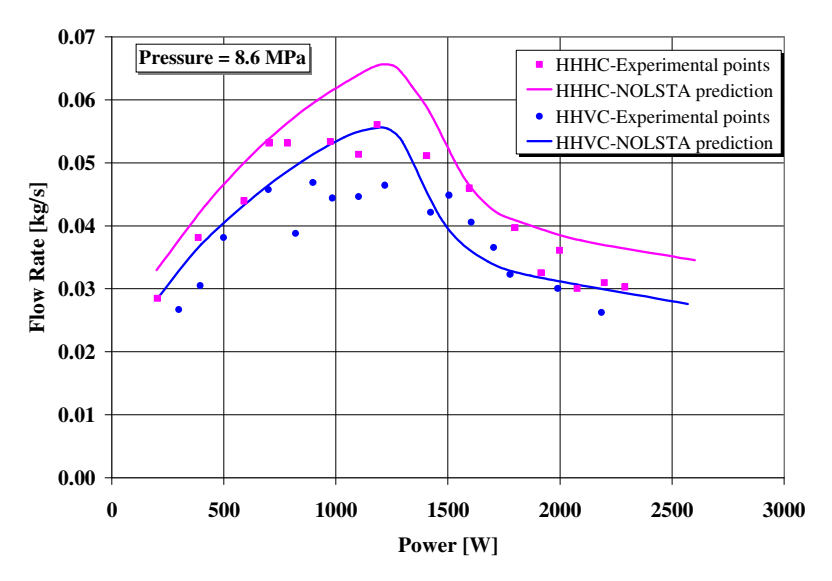


Figure 5. Steady state flow rate at 8.6 MPa in HHHC and HHVC configurations

In addition to experiments in steady state conditions, transient tests were also performed. During these tests, instabilities were observed only for the HHHC orientation, while all the other orientations were found to be fully stable. However, even for the HHHC orientation, both the subcritical and the supercritical regions beyond the pseudo-critical region were found to be most stable, because instabilities were observed only for a narrow window in the pseudo-critical region at low secondary coolant flow rates (20 lpm or less).

The experiments in which the instabilities were detected are the following:

- a) start-up from rest;
- b) power raised or lowered from a stable steady state;
- c) large power decrease from a stable steady state.

Typical instabilities observed for start-up from rest are shown in Figure 6.

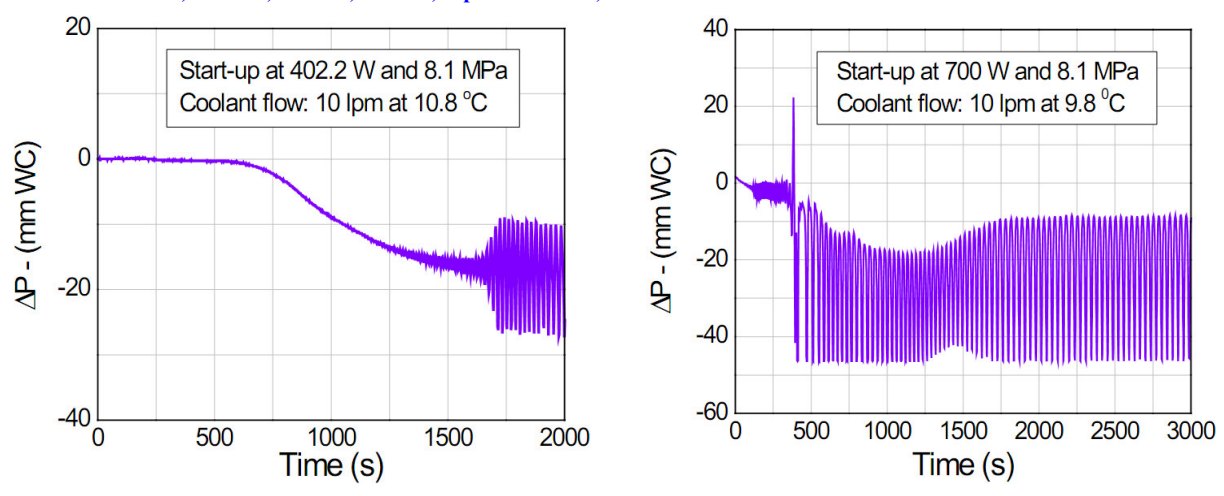


Figure 6. Start-up from rest at different powers

In the case of power raised or decreased starting from the steady state conditions, typical observed instabilities at 9.1 MPa (though they were observed also at lower pressures) are shown in Figure 7 for 500 W and 800 W with 10.1 and 15 lpm of secondary cooling flow rates. An interesting feature of the oscillations is that the inlet temperature remains almost constant while only the outlet temperature is oscillating. On the other hand, the approximate equality between the time period of heater outlet temperature oscillations and the loop circulation time calculated by NOLSTA code [8] points to a Welander-like mechanism [9] for development of instability.

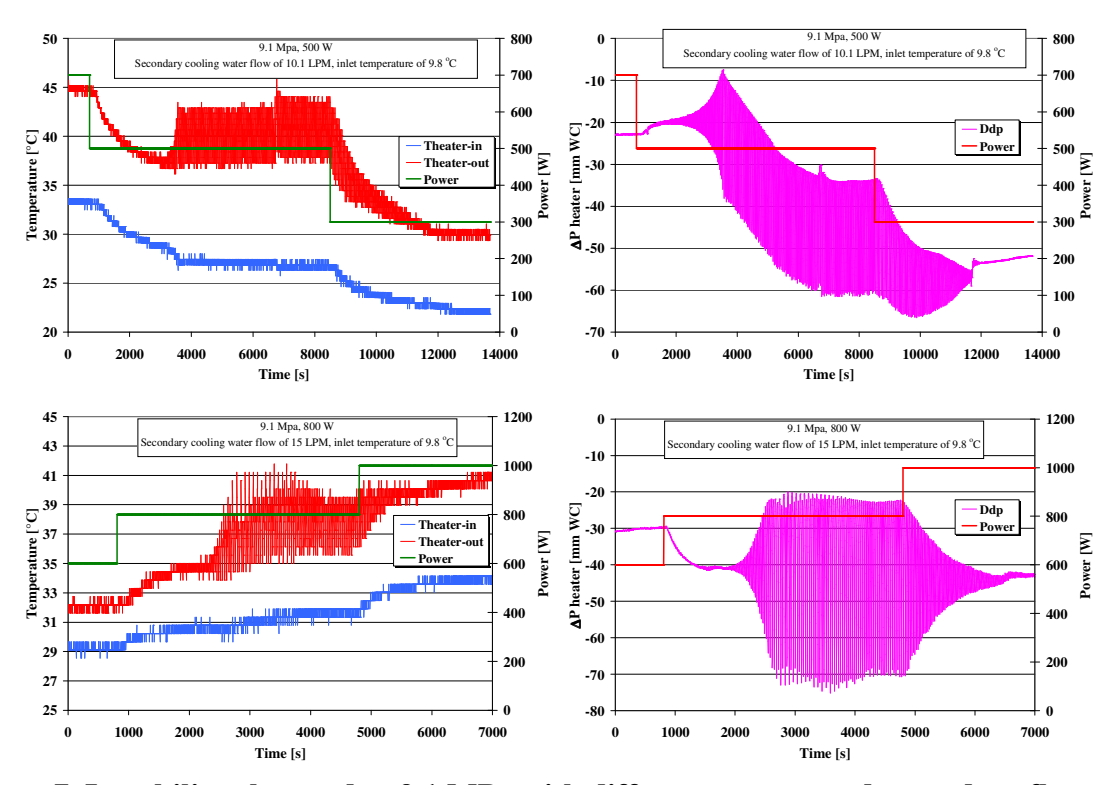


Figure 7. Instability observed at 9.1 MPa with different powers and secondary flow rates

4. Adopted CFD codes and models

The use of CFD tools has proven to give a valuable support in getting understanding of natural circulation physical phenomena. Recently, in a joint investigation of single-phase natural circulation phenomena by BARC and the University of Pisa [10] only a CFD model, thanks to its 3-D nature, was able to provide a physically reasonable prediction of the unidirectional pulsating instabilities in HHHC configuration of a single-phase natural circulation loop installed at BARC. Indeed, at the origin of the behaviour there was a slight thermal stratification occurring in the horizontal pipes which 1-D codes with cross-section averaged variables obviously could not predict.

For this reason, two different computational fluid-dynamic codes Fluent [5] and STAR-CCM+ [6] have been adopted for simulating the system static and dynamic characteristics of the experimental facility of BARC in different configurations. The reason for using two CFD codes, instead of a single one, is due to the fact that it was considered interesting comparing their results because the codes use different spatial meshes and different numerical algorithms and turbulence models. Both Fluent and STAR-CCM+, as many other available CFD codes, make use of the finite volume discretisation technique. In this aim, the solution domain is subdivided into a number of small volumes of appropriate size, corresponding to the cells of the computational grid, and then the integral versions of the transport equations are applied to each control volume. In both cases the RANS approach was used.

In setting up the spatial discretisation, the symmetry of the SPNCL facility with respect to a middle vertical plane made possible to model only a half of the loop. This allowed to reduce the number of finite volumes and, obviously, to save computational time. For the Fluent code a structured mesh was adopted: 28 non uniform cells were defined on the diameter and 20 cells are used on the outer circumference. Of the overall 230 cells present in the cross section, 150 are used to mesh the fluid region and 80 for the solid region, making use of a conjugated heat transfer approach.

Sketches of the spatial discretisation adopted for Fluent are reported in Figure 8.

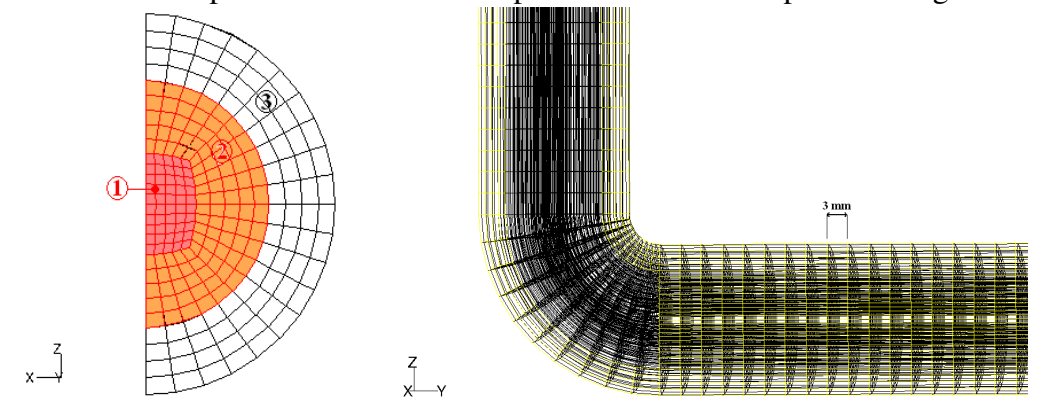


Figure 8. Spatial discretisation adopted for the FLUENT code

For the STAR-CCM+ code, the generation of the mesh was automatically obtained by the built-in mesher of the code, after selecting appropriate models (polyhedral nodes in the core and prism layers at the wall) with a target size of 2 mm. The result was a polyhedral mesh in the center of the fluid region, 5 prism layers near the wall, and 3 layers adopted to discretize the solid region (Figure 9).

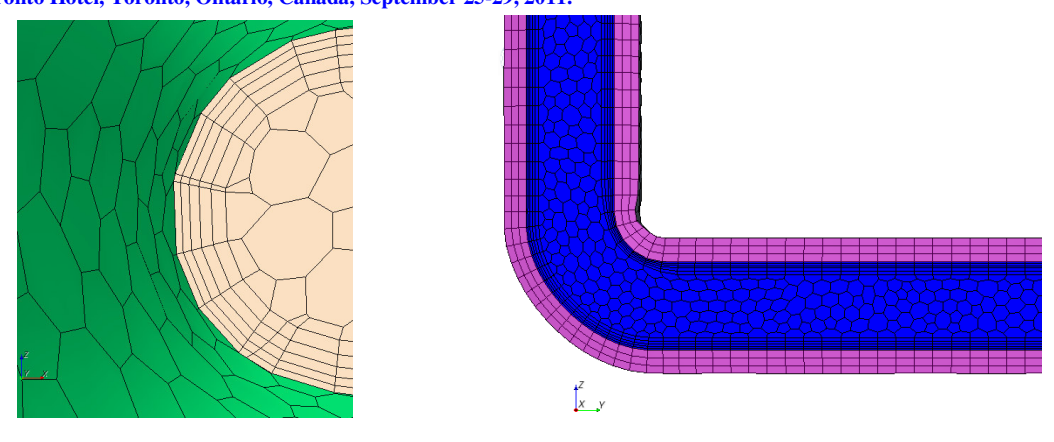


Figure 9. Spatial discretisation adopted for the STAR-CCM+ code

In the case of the Fluent code, the most convenient way to assign the properties of CO₂ at a given pressure as a function of temperature was found to be in the form of a piece-wise linear approximation with 30 points, which is the maximum number allowed by the code. Particular attention was paid in order to match the trend of sharply varying properties, as specific heat and thermal conductivity, by a linear interpolation of the data calculated by the NIST package [11]. Obviously, also the check of a good interpolation of the other fluid properties was made (Figure 10a).

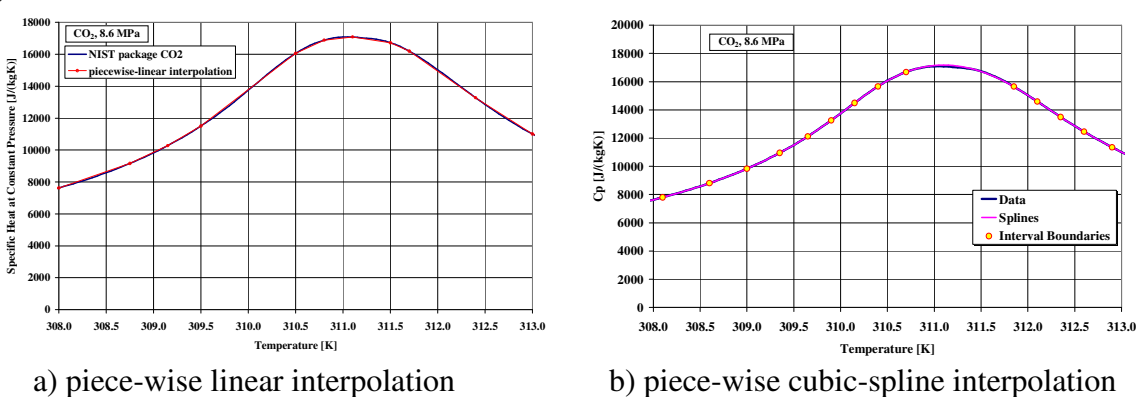


Figure 10. Detail of piece-wise linear and cubic-spline interpolation of CO₂ specific heat around the pseudocritical temperature (311.05 K) at 8.6 MPa

On the other hand, with the STAR-CCM+ code, the fluid properties were provided in the form of cubic splines generated with a purposely developed code written in FORTRAN 77 (Figure 10b). The cubic spline interpolation is certainly more accurate than the linear one and also ensures to preserve the continuity of first and second derivatives across the whole range of interpolation. Moreover, the unrestricted number of intervals through which the fluid properties can be assigned in STAR-CCM+, made it possible to get a very close interpolation with a wider temperature range, 220 – 600 K, than in the case of Fluent.

The turbulence models adopted in both codes were of the k-ɛ type, equipped with wall functions (or the "all-y" approach) capable to account also for pipe roughness. The presence of prism layers close to the wall was purposely selected in order to obtain enough detail in phenomena representation, though the wall function treatment is intrinsically incapable to deal with heat transfer enhancement and deterioration observed in the case of supercritical fluids.

5. Obtained Results

Only the HHHC configuration of the loop was considered in the analyses. The most important operating conditions to be considered in the simulations are the pressure of the loop and the secondary heat transfer coefficient assumed at the cooler. In our case, a pressure of 8.6 MPa was chosen for steady-state conditions, as specified in experiments, while the secondary heat transfer coefficient was estimated equal to 850 W/(m²K), though the indicative value calculated with Dittus-Boelter formula was a bit lower (567 W/(m²K)). This greater value tried to account for thermal and fluid-dynamic entry length effects and was selected after discussion with experimentalists.

The heat transfer coefficient with the environment was set equal to $2 \text{ W/(m}^2\text{K})$, because it takes into account also the thermal resistance of the loop insulation with the three inches of ceramic mat. A tube roughness equal to 2.5×10^{-5} m was chosen basing on the values of a typical roughness of stainless steel tubes.

In Figure 11a, the flow vs. power curves obtained by the CFD codes are reported. Fluent predictions match the experimental results fairly well, with STAR-CCM+ providing a slightly different behaviour, giving an idea of the consequences of small differences in the adopted models. However, both CFD codes predict a sharp flow rate decrease passing from the buoyancy dominated to the friction dominated region (on the left and the right of the maximum flow rate, respectively) which is not found in the experimental data. This behaviour can be explained with the strong degradation in heat transfer at the cooler evaluated by the codes when the temperature crosses the pseudo-critical level at cooler inlet.

In Figure 11b the heater inlet and outlet temperatures are reported as calculated by Fluent. It can be observed that the sharp flow decrease occurs when the heater inlet temperature exceeds the pseudocritical one. As a consequence, the temperature difference across the heater increases sharply as well as the slope of the temperature curves. Since the loop is insulated and the mean temperatures of the supercritical CO₂ are not so far from the environmental temperature level, the heat losses fraction calculated is generally less than 5%. However, it must be considered that "heat losses" become "heat sources" at low power when the heater outlet temperature is below the environmental temperature. For this reason, the codes predict flow circulation even when the heater is switched off, as observed in the experiments, being the environment the thermal source in the loop.

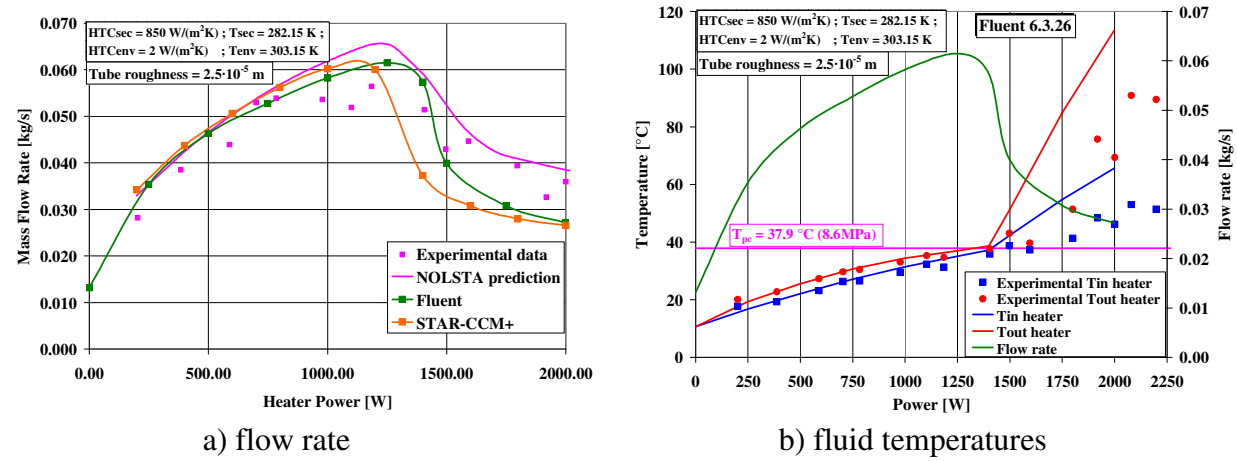


Figure 11. Steady-state flow rate and fluid temperatures vs. heating power as predicted by the Fluent and the STAR-CCM+ codes

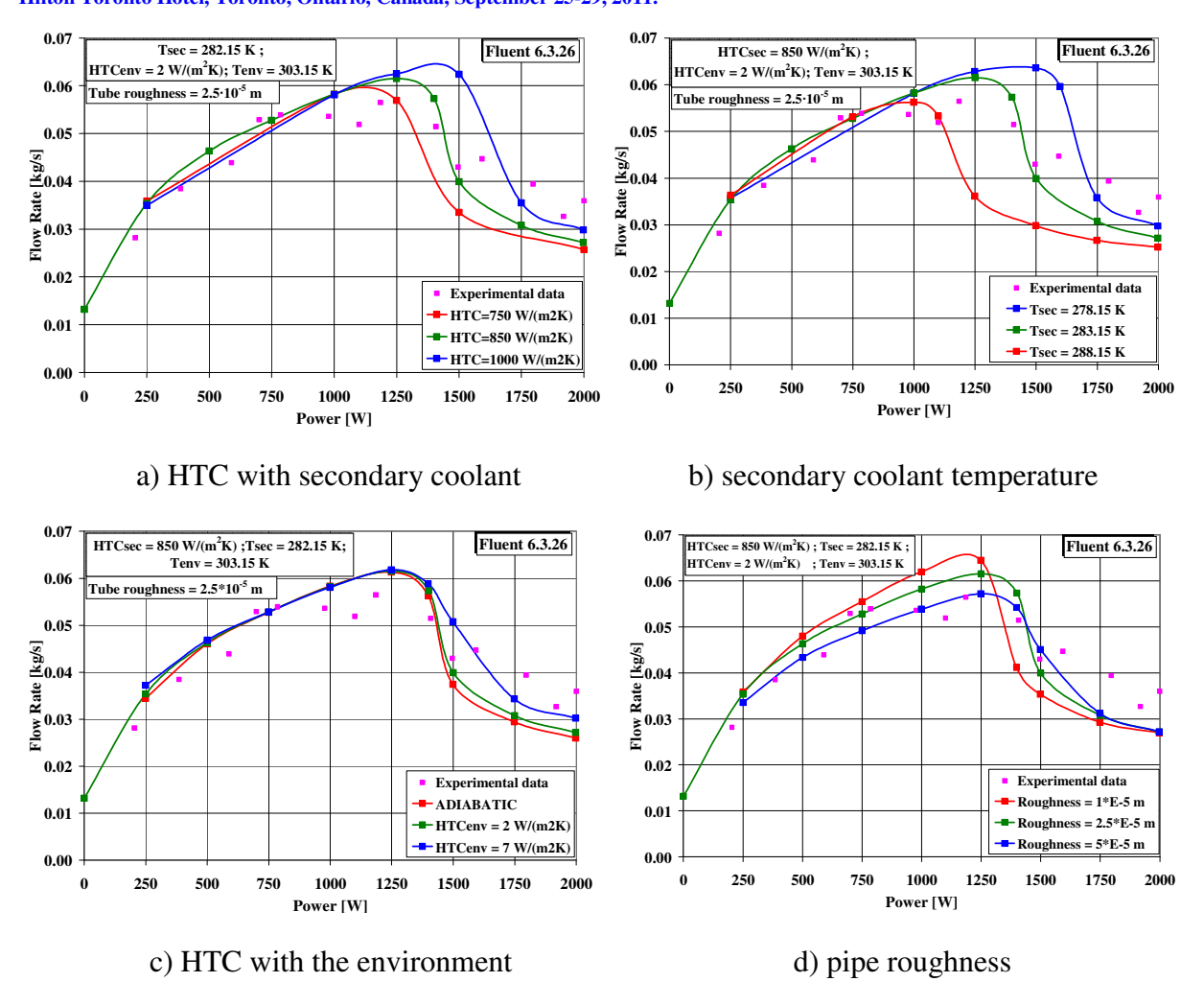


Figure 12. Sensitivity analyses concerning the effect of different parameters on the flow rate vs. power curve performed by the Fluent code

Sensitivity analyses were performed on different modelling parameters in order to check their effect on the flow rate vs. power curve. The results obtained by these analyses, whose main results are reported in Figure 12, show that the power at which a maximum occurs in flow rate critically depends on heat transfer to the secondary coolant and to the outer environment, as well as on hydraulic impedance. In light of these results, the slight differences obtained by Fluent and STAR-CCM+ for the base calculation cases can be easily understood as the result of slightly different assumptions in modelling these phenomena.

By the way, it must be recognised that the phenomena occurring at powers beyond the one resulting in the maximum flow rate as a function of power involve a sudden deterioration of heat transfer to the secondary coolant, occurring when both the cold and the hot legs of the loop have temperatures exceeding the pseudo-critical threshold. In fact, in such a case a rapid deterioration of heat transfer is experienced because the fluid changes from liquid-like to gas-like and this deterioration is reinforced by the consequent increase of fluid temperature needed to preserve the energy balance from the heater to the secondary fluid. These processes are schematically described in Figure 13, presenting in a logical way the occurrence of the involved phenomena.

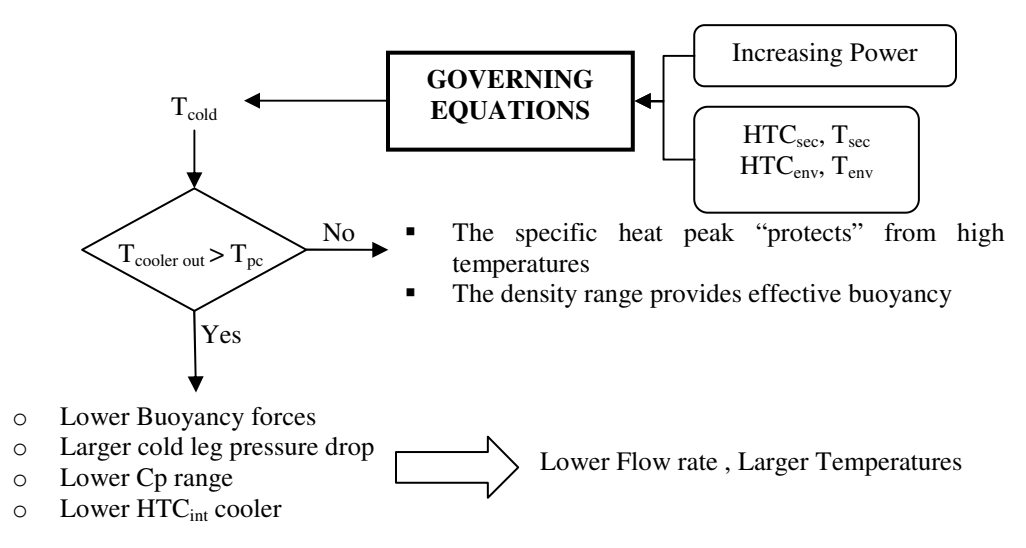


Figure 13. Logical flowchart of the effects leading to flow rate decrease after the maximum

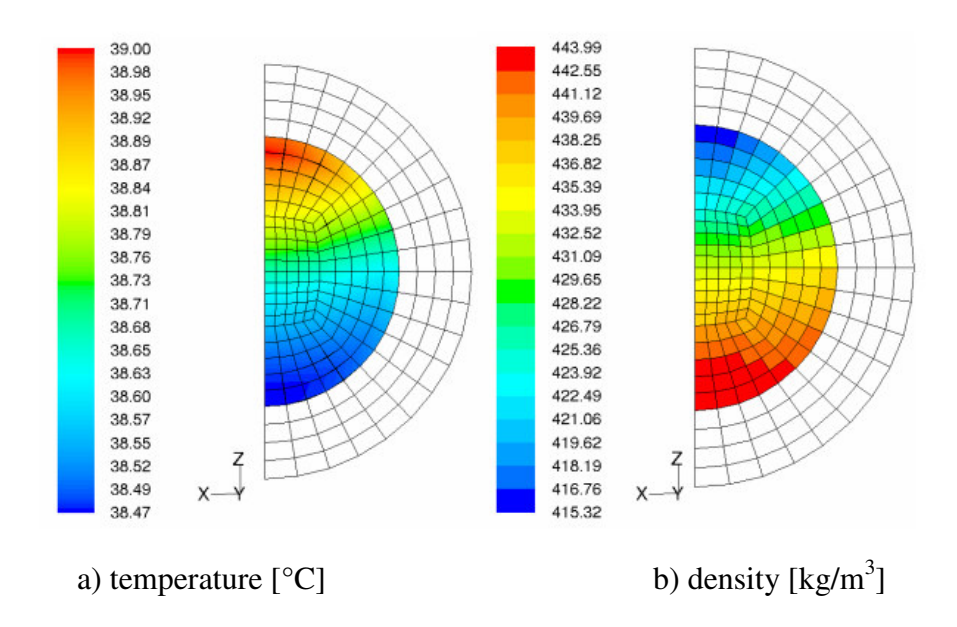


Figure 14. Temperature and density contour plots obtained by Fluent close to the location of T15 and T16 thermocouples at a power of 1400 W

It is interesting to note that the CFD codes have the capability to highlight details of these phenomena that are much richer than it is possible to observe by classical 1D tools. In fact, though the diameter of the loop is relatively small, thermal stratification phenomena are predicted by the codes, which have certainly a role in the observed degradation of heat transfer to the outer environment. Such stratification processes are described in Figure 14 referred to the heater outlet in a specific operating condition.

Despite of the good results obtained by the steady-state calculations, actually it was not possible to predict by either CFD code the unstable behaviour observed in experimental conditions, previously described in Figure 7. In fact, it was found that unstable behaviour could be predicted only by decreasing the density of the loop wall heat structures by a factor 10. Moreover, the unstable behaviour observed in such simulations was substantially different from the one observed in the experimental tests. The simulated behaviour for a start-up and a power

decrease transient is shown in Figure 15, highlighting the presence of flow reversals, not observed in experiments.

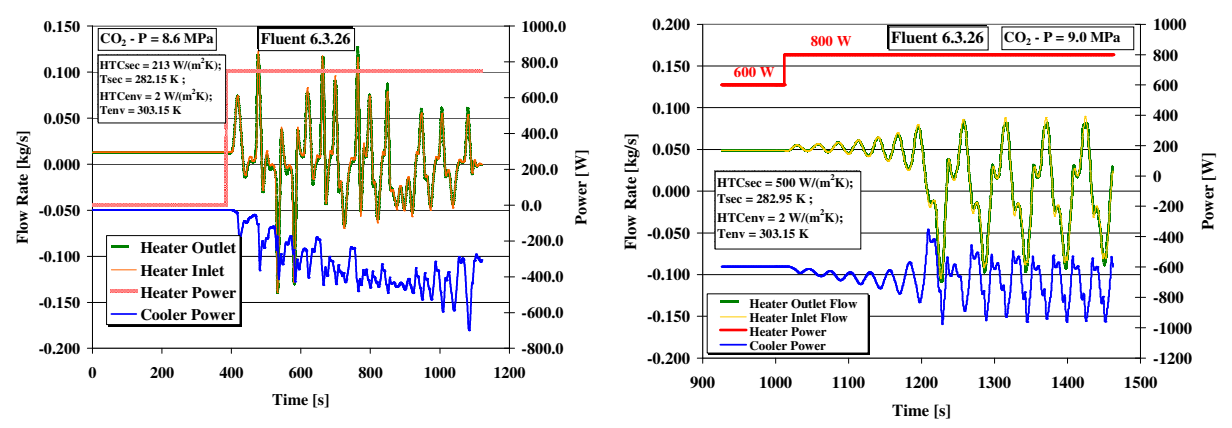


Figure 15. Flow rates and powers in start-up and power increase simulations (walls with reduced density)

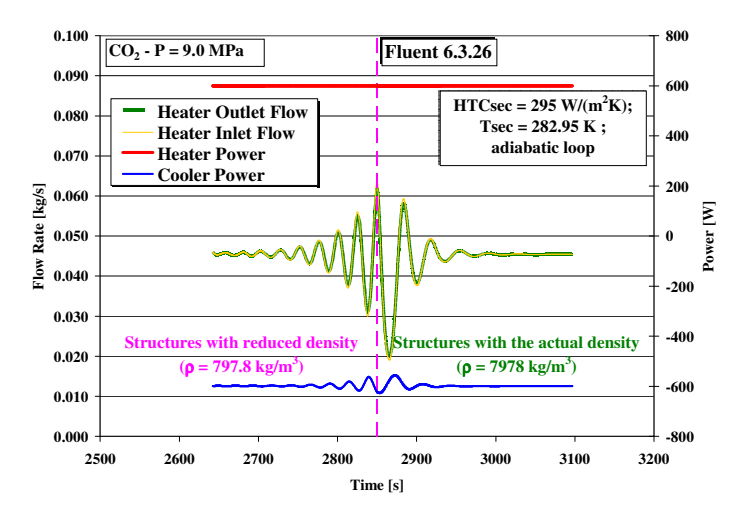


Figure 16. Effect of the heat structures density on unstable behaviour

In order to ascertain that the heat capacity of the heat structures was mainly responsible for the observed damping in dynamic behaviour, specific calculations were also run staring with a (tenfold) reduced heat structure density, then restoring the structure density to its original value. An example of results obtained by such analyses is reported in Figure 16, showing that the behaviour is initially observed to be oscillatory, while after restoring the physically reasonable value of structure density the obtained flow oscillations are rapidly damped.

6. Conclusions

The results obtained in the application of the two CFD codes in the analysis of the experimental data collected by BARC with the SPNCL facility with carbon dioxide as a working fluid are quite encouraging. In particular, the main steady-state phenomena observed in the experiments could be reproduced both in the buoyancy and in the friction dominated regions of the flow vs. power characteristic of the loop.

The phenomenon of transition from the first to the second of the two operating regions could be clearly understood on the basis of the results provided by the codes. The effect of different operating parameters and modelling assumptions on the location of the maximum of

flow rate as a function of power was assessed by several calculations, highlighting the main contributors to the specific observed trends, also allowing to suggest an explanation for the slight differences observed between the results of the two codes.

Even if the instabilities observed in the experiments could not be predicted by the codes, suggesting the need for refinements in the representation of loop details, the present application of CFD models to natural circulation of supercritical fluids is quite promising and provided the chance to set up methodologies of analysis with both Fluent and STAR-CCM+ which will be used in the future for further model assessment.

7. References

- [1] K. Fischer, T. Schulenberg, E. Laurien, Design of a supercritical water-cooled reactor with a three-pass core arrangement, Nuclear Engineering and Design, Volume 239, Issue 4, April 2009, Pages 800-812.
- [2] Jaewoon Yoo, Yuki Ishiwatari, Yoshiaki Oka, Jie Liu, Conceptual design of compact supercritical water-cooled fast reactor with thermal hydraulic coupling, Annals of Nuclear Energy, Volume 33, Issues 11-12, August 2006, Pages 945-956.
- [3] R. Duffey, L.K.H. Leung and I. Pioro, Design Principles and Features of Supercritical Water-cooled Reactors to Meet Design Goals of Generation-IV Nuclear Reactor Concepts, Technical Meeting On Heat Transfer, Thermal-Hydraulics And System Design For Supercritical Water, Pisa, Italy, July 5-9, 2010.
- [4] S. Lomperski, D. Cho, R. Jain, M.L. Corradini, Stability of a natural circulation loop with a fluid heated through the thermodynamic pseudocritical point. In: Proceedings of ICAPP'04, Pittsburgh, PA, USA, June 13–17, Paper 4268.
- [5] Fluent, 2006. FLUENT 6.3.26 User Guide.
- [6] STAR-CCM+, web-site http://www.cd-adapco.com/products/STAR-CCM_plus/
- [7] P.K. Vijayan, M. Sharma, D.S. Pilkhwal and D. Saha, Steady State and Stability Characteristics of a Supercritical Pressure Natural Circulation Loop (SPNCL) with CO₂, Annual Progress Report on Heat Transfer, Pressure Drop and Stability Studies for Supercritical Natural Circulation Systems, Research Contract 14344/R2, BARC, Dec. 2010.
- [8] Manish Sharma, P.K. Vijayan, D.S. Pilkhwal, D. Saha and R.K. Sinha, "Linear and non-linear stability analysis of a supercritical natural circulation loop", *ASME Journal of Engineering for Gas Turbines and Power*, October 2010, Vol. 132/ 102904-1.
- [9] P. Welander, 1967, On the oscillatory instability of a differentially heated fluid loop. J. Fluid Mech. 29, 17–30.
- [10] D.S. Pilkhwal, W. Ambrosini, N. Forgione, P.K. Vijayan, D. Saha, J.C. Ferreri, Analysis of the unstable behaviour of a single-phase natural circulation loop with one-dimensional and computational fluid-dynamic models, *Annals of Nuclear Energy* 34 (2007) 339–355.
- [11] NIST, 2002. Reference Fluid Thermodynamic and Transport Properties REFRPROP. Lemmon, E.W., McLinden, M.O., Hurber, M.L. (Eds.), NIST Standard Reference Database 23 (Software and Source), V. 7.0, U.S. Department of Commerce.

Acknowledgements

The support of the International Atomic Energy Agency (IAEA), through the Research Agreement No. 14272, is acknowledged in connection with the Co-ordinated Research Project in 'Heat transfer behaviour and thermo-hydraulics code testing for super-critical water cooled reactors (SCWRs)'. CD-Adapco, in the person of Dr. Emilio Baglietto, is acknowledged for making possible this research.